https://doi.org/10.5194/egusphere-2026-5353
Preprint. Discussion started: 29 September 2026

Unappreciated role of sulfate radicals in the aqueous aging process of methoxyphenols derived from biomass burning

Ru Chen[1], Xiang Li[1], Xinjiao Huang[1], Yanli Ge[2,*], Ruiyu Li[3,4], Tianzeng Chen[3,4], Zhengzheng Yang[1], Lu Fan[1], Mingchao Sun[1], and Changgeng Liu[1,*]

[1]College of Chemistry and Materials Science, Sichuan Normal University, Chengdu 610066, China

[2]State Environmental Protection Key Laboratory of Quality Control in Environmental Monitoring, China National Environmental Monitoring Centre, Beijing, 100012, China

[3]Laboratory of Atmospheric Environment and Pollution Control, Research Center for Eco-Environmental Sciences, Chinese Academy of Sciences, Beijing 100085, China

[4]University of Chinese Academy of Sciences, Beijing 100049, China

*Corresponding author.

E-mail address: Yanli Ge (geyl@cnemc.cn) and Changgeng Liu (changwyx@sicnu.edu.cn)

Abstract: Methoxyphenols are widely acknowledged tracers of biomass burning emissions, undergo complex chemical transformations in atmospheric aqueous environments that significantly modulate aerosol properties. The role of sulfate radicals ($SO_4^{\bullet-}$), the highly potent electrophiles prevalent in cloud and fog waters, remains poorly constrained. Herein, we investigated the aqueous-phase kinetics and aqueous secondary organic aerosol (aqSOA) formation of three representative methoxyphenols containing different substituents, namely vanillic acid (VAA), vanillin (VAL), and

https://doi.org/10.5194/egusphere-2026-5353
Preprint. Discussion started: 29 September 2026

coniferyl aldehyde (CFA), upon oxidation by $SO_4^{\bullet-}$. The determined second-order rate constants for VAA, VAL, and CFA with $SO_4^{\bullet-}$ were in the range of (2.40-3.37) × 10^9 M^{-1} s^{-1}, revealing that side-chain substituents critically govern reactivity through π-electron density modulation. These reactions efficiently generated aqSOA with maximum mass yields of 63.12%-70.49%, characterized by high oxidation degree comparable to that of atmospheric low-volatility oxygenated organic aerosols (LV-OOA). Notably, the oxidation process driven the generation of humic-like substances (HULIS) with pronounced light-absorbing capabilities in the near-ultraviolet and visible regions, thereby contributing to atmospheric brown carbon. Furthermore, the oxidation products exhibited significantly elevated oxidative potentials compared to their precursors, posing enhanced health risk. Our findings identify $SO_4^{\bullet-}$-initiated aqueous chemistry as a critical yet previously overlooked pathway that transforms biomass burning emissions into toxic and light-absorbing secondary aerosols. Therefore, it is necessary to incorporate $SO_4^{\bullet-}$-related processes into atmospheric models to accurately predict air quality and climate forcing.

Keywords: Substituted methoxyphenols, Sulfate radicals, Aqueous-phase reaction, Rate constant, Secondary organic aerosol, Optical property, Oxidation potential

https://doi.org/10.5194/egusphere-2026-5353
Preprint. Discussion started: 29 September 2026

1 Introduction

Sulfate radicals ($SO_4^{\bullet-}$) are important atmospheric oxidants that exclusively exist in atmospheric aqueous media (Herrmann et al., 2010, 2015). Its estimated average concentration within cloud droplets and deliquescent particles spans 3.6×10^{-13} to 2.3×10^{-15} mol L^{-1}, which is comparable to those of hydroxyl radicals ($^{\bullet}OH$) and nitrate radicals ($NO_3^{\bullet}$) (Herrmann et al., 2010). Given its high oxidation potential (2.5-3.1 V) and persistent reactivity over a broad pH range (2-9) (Liu et al., 2018). $SO_4^{\bullet-}$ can efficiently degrade a wide variety of soluble organic pollutants in atmospheric aqueous environments, including aromatics, alcohols, carboxylic acids, ethers, etc. (Herrmann et al., 2010, 2015; Rudziński and Szmigielski, 2019; Wojnárovits and Takács, 2019), and their corresponding second-order rate constants fall within the range of 10^7 to 10^9 M^{-1} s^{-1}. In the past, it is well established that $SO_4^{\bullet-}$ is primarily generated via the autoxidation chain reaction of sulfur dioxide, alongside minor formation pathways involving the activation of sulfate or bisulfate ions by $^{\bullet}OH$, $NO_3^{\bullet}$, or iron species (Herrmann et al., 2010). In recent years, additional formation pathways of $SO_4^{\bullet-}$ in atmospheric aqueous media have been uncovered, chiefly including irradiation of sulfate-containing organic aerosols, $^{\bullet}OH$-initiated oxidation of organosulfates (OSs), and autocatalytic reactions of sulfate anion (SO_4^{2-}) (Cope et al., 2022; Kwong et al., 2018; Pan et al., 2019). To date, the potentially critical role of $SO_4^{\bullet-}$ remains poorly elucidated. Therefore, more systematic investigations into $SO_4^{\bullet-}$-initiated reactions of representative organic pollutants are urgently required, particularly to fill the gaps

https://doi.org/10.5194/egusphere-2026-5353
Preprint. Discussion started: 29 September 2026

regarding the corresponding kinetics and secondary organic aerosol (SOA) formation.

Methoxyphenols are broadly acknowledged as reliable tracers of biomass burning emissions (Nolte et al., 2001; Liu et al., 2022). Formed during the pyrolysis process of lignin, such species have been extensively identified within atmospheric gas, particulate, and aqueous phases (Liu et al., 2022). 2-Methoxyphenol and 2,6-dimethoxyphenol represent the basic structures of methoxyphenols, with their Henry's law constants ranging from 10^3 to 10^4 M atm^{-1} (Arciva et al., 2022). In contrast, substituted methoxyphenols exhibit far larger Henry's law constants (10^6-10^9 M atm^{-1}) and partition substantially into atmospheric aqueous phase, even under aerosol liquid water conditions (Mcfall et al., 2020). In addition, the measured concentration of methoxyphenols in fog water is 3-4 times higher than the values predicted by Henry's law (Kitanovski et al., 2014). Therefore, aqueous-phase reactions of these compounds constitute a critical pathway for atmospheric chemical transformation, especially in regions affected by biomass burning. In recent years, aqueous-phase reactions of methoxyphenols with $^{\bullet}OH$ and triplet excited states ($^3C^*$) have garnered growing attention within the research community. The existing relevant work has primarily reported reaction rate constants, aqueous-phase SOA (aqSOA) formation, oxidation products, and the underlying mechanisms (An et al., 2020; Arciva et al., 2022; Chen et al., 2020; Huang et al., 2018; Lai et al., 2025; Li et al., 2021; Loisel et al., 2021; Ma et al., 2021; Pang et al., 2019; Smith et al., 2014, 2015; Tang et al., 2020; Yang et al., 2023, 2024; Ye et al., 2020; Yu et al., 2016). However, aqueous-phase reactions of substituted

https://doi.org/10.5194/egusphere-2026-5353
Preprint. Discussion started: 29 September 2026

methoxyphenols with $SO_4^{\bullet-}$ have been scarcely reported even if they have potential coexistence aqueous environment in the atmosphere (Herrmann et al., 2010; Kitanovski et al., 2014). In particular, the corresponding kinetic data and possible aqSOA formation are not well characterized.

To address the aforementioned knowledge gaps, here we investigated aqueous-phase reactions of $SO_4^{\bullet-}$ with three representative methoxyphenols containing different substituents on the 2-methoxyphenol backbone, namely vanillic acid (VAA), vanillin (VAL), and coniferyl aldehyde (CFA), focusing on kinetics, aqSOA mass yields, optical properties, and oxidation potentials. The findings of this work provide new insights into the aqueous-phase chemical transformation of methoxyphenols in the atmosphere and furnish updated kinetic and aqSOA mass yield datasets for application in atmospheric modeling.

2 Experimental section

2.1 Aqueous-phase reactions

Fresh solution of 0.3 mM methoxyphenol sample was prepared using deionized water. 300 mL of sample solution was introduced into a 500 mL cylindrical glass reactor (Fig. S1), and its initial pH was adjusted to 2 by diluted sulfuric acid and sodium hydroxide. Subsequently, 50 mM peroxydisulfate (PDS, $Na_2S_2O_8$) was added and applied to produce $SO_4^{\bullet-}$ in this system via gently thermal decomposition at 50 °C. Meanwhile, 50 mM *tert*-butyl alcohol (TBA) was added in order to prevent the possible interference of $^{\bullet}OH$. Lastly, the aqueous-phase reactions of methoxyphenols with $SO_4^{\bullet-}$

https://doi.org/10.5194/egusphere-2026-5353
Preprint. Discussion started: 29 September 2026

were initiated. The solution was first stirred at 450 rpm for 2 min, after which stirring was maintained at 50 rpm for the entire duration of the experiment. At predetermined time intervals, solution samples were collected for the following analysis. In addition, the possible impacts of temperature and ion strength on aqueous-phase reactions were not taken into account in this work and discussed in detail in the Supplement.

2.2 Relative rate method

The relative rate method was used to determine the second-order rate constants of VAA, VAL, and CFA in the aqueous-phase reactions with $SO_4^{\bullet-}$. The corresponding equation is listed as follows: $\ln(\frac{C_{M0}}{C_{Mt}})=\frac{k_{2,M}}{k_{2,R}}\ln(\frac{C_{R0}}{C_{Rt}})$, where C_{M0} and C_{R0} are the initial concentrations of methoxyphenol sample and reference compound, respectively; C_{Mt} and C_{Rt} are their concentrations at reaction time *t*. $k_{2,M}$ and $k_{2,R}$ are the second-order rate constants of methoxyphenol sample and reference compound. In this work, ferulic acid was adopted as the reference compound, which is a typical kind of methoxyphenols with a second-order rate constant of 3.2×10^9 M^{-1} s^{-1} toward $SO_4^{\bullet-}$ (Herrmann et al., 2010). In the experiments, methoxyphenols and ferulic acid were both used at an identical initial concentration of 0.3 mM, with all other experimental conditions consistent with those described in the preceding section.

2.3 Analytical methods

A double-beam UV-vis spectrophotometer (M9, Shanghai Mapada, China) was employed to record the UV-vis absorption spectra of solution samples within the wavelength range of 200-800 nm at predetermined intervals. Deionized water was used

https://doi.org/10.5194/egusphere-2026-5353
Preprint. Discussion started: 29 September 2026

as reference solution. During data processing, the signals of absorption spectra were corrected to eliminate the possible background interferences caused by TBA and inorganics in the solution. The fluorescence spectrophotometer (F-7000, Hitachi, Japan) was adopted to conduct three-dimensional excitation-emission matrix (EEM) fluorescence spectral scanning of solution samples. Its emission wavelength scanning range was 220-700 nm with a scanning step size of 5 nm, and corresponding excitation wavelength scanning range was 200-600 nm with a scanning step size of 10 nm. The scanning speed was 2400 nm min^{-1}. The concentrations of methoxyphenol sample and ferulic acid were measured by gas chromatography-mass spectrometer (GC-MS) analysis. Before analysis, solution samples were extracted using CH_2Cl_2 and then derivatized by *N*,*O*-bis(trimethylsilyl)trifluoroacetamide. Humic-like substances (HULIS) were isolated from reaction products using solid-phase extraction cartridges (CNW Poly-Sery HLB) and quantified via high performance liquid chromatography (HPLC) analysis. In addition, an improved dithiothreitol (DTT) assay method was adopted to analyze the oxidation potential of reaction products (Li et al., 2022). 2-Nitro-5-thiobenzoic acid (TNB) produced from the reaction between DTT and 5,5'-dithiobis (2-nitrobenzoic acid) (DNTB) has a characteristic absorption at 412 nm. Thus, the consumption rate of DTT can be calculated by its corresponding changes in absorbance. An Aerodyne high-resolution time-of-flight aerosol mass spectrometer (HR-ToF-AMS) was applied to characterize the mass concentration and chemical composition of aqSOA (Decarlo et al., 2006). The mass data acquired from the HR-ToF-AMS were analyzed

https://doi.org/10.5194/egusphere-2026-5353
Preprint. Discussion started: 29 September 2026

using the toolkit SQUIRREL 1.57I/PIKA 1.61I version in Igor Pro version 6.37. Detailed descriptions of the UV-vis, EEM, GC-MS, DTT, and HULIS measurements, HR-ToF-AMS analysis, and the calculation of aqSOA mass yields are provided in the Supplement.

3 Results and discussion

3.1 Rate constants

The second-order rate constants for VAA, VAL, and CFA in the aqueous-phase reactions with $SO_4^{\bullet-}$ were determined by the relative rate method in this work. As shown in Fig. 1, data points were well fitted using a linear regression ($R^2 > 0.97$). Table 1 lists the slopes, rate constants, and corresponding atmospheric lifetimes (τ). The uncertainties of the slopes (i.e., $k_{2,M}/k_{2,R}$) correspond to the standard deviations obtained from linear regression analysis. As shown in Table 1, the second-order rate constants for VAA, VAL, and CFA were determined to be $(2.40 \pm 0.19) \times 10^9$ M^{-1} s^{-1}, $(2.56 \pm 0.10) \times 10^9$ M^{-1} s^{-1}, and $(3.37 \pm 0.22) \times 10^9$ M^{-1} s^{-1}, respectively. This observation indicates that the rate constants are strongly affected by variations in the side-chain substituents of 2-methoxyphenol backbone, as detailed below. Table 2 summarizes $k_{2,M}$ values for aqueous-phase reactions of methoxyphenols with $SO_4^{\bullet-}$, $^{\bullet}OH$, and $^3C^*$, compiled from published literatures. The $k_{2,M}$ values of methoxyphenols reacting with $SO_4^{\bullet-}$ and $^3C^*$ are comparable and on the order of 10^9 M^{-1} s^{-1}, approximately 2-5 times lower than those for reactions with $^{\bullet}OH$. In addition, the $k_{2,M}$ values obtained in this work are comparable to those reported for other aromatic compounds (e.g., nitrophenol and

https://doi.org/10.5194/egusphere-2026-5353
Preprint. Discussion started: 29 September 2026

benzaldehyde) reacting with $SO_4^{\bullet-}$ and $NO_3^{\bullet}$ (Herrmann et al., 2010). Therefore, $SO_4^{\bullet-}$-initiated degradation reasonably serves as an important transformation pathway of methoxyphenols in atmospheric aqueous environments.

$SO_4^{\bullet-}$ is an effective electrophilic oxidant and capable of undergoing single electron transfer (SET), addition to a double bond, and hydrogen abstraction from aliphatic parts of organic molecules (Luo et al., 2017; Neta et al., 1988; Tong et al., 2020; Wojnárovits and Takács, 2019). During reactions with organic molecules containing C=C bond, radical adducts may potentially form, but no such adducts have been detected to date (Paul et al., 2014; Wojnárovits and Takács, 2019). However, SET is overwhelmingly dominant mechanism for its reactions with phenolic aromatics, simultaneously accompanied by the formation of SO_4^{2-} and radical cations of aromatic molecules (Luo et al., 2017; Tong et al., 2020; Wojnárovits and Takács, 2019). Therefore, the reaction rate constant strongly depends on the π-electron density and the extent of π-conjugation of organic molecules. In this work, VAA, VAL, and CFA share an identical 2-methoxyphenol backbone, and their structural differences arise from distinct side-chain substituents attached to the same C position on the benzene ring. CFA bears a −CH=CH−CHO side chain with a Hammett substituent constant (σ_p) of approximately +0.31, which forms an extended conjugated system spanning the aromatic ring, C=C bond, and terminal −CHO group (Gould, 1959). The expanded delocalization of π electrons, together with the reactive C=C bond serving as an additional electrophilic attack site, leads CFA to become most reactive toward $SO_4^{\bullet-}$. By contrast, VAA and

https://doi.org/10.5194/egusphere-2026-5353
Preprint. Discussion started: 29 September 2026

VAL possess $^{-}$COOH and $^{-}$CHO side chains, respectively. Both substituents act as strong electron-withdrawing groups, with comparable σ_p values (+0.45 for $^{-}$COOH and +0.42 for $^{-}$CHO) (Jaffé, 2002), and markedly reduce the π-electron density of the aromatic ring (Chataigner et al., 2007; Pang et al., 2019). Consequently, the SET pathway initiated by $SO_4^{\bullet-}$ is suppressed, which results in low and similar rate constants for VAA and VAL. Consistent with these observations, Li et al. (2021) and He et al. (2019) have recently reported that electron-withdrawing substituents (e.g., $^{-}$COOH) on methoxyphenols markedly reduce their reactivity toward $^{\bullet}$OH under aqueous-phase conditions, thereby decreasing the corresponding rate constants. On the contrary, electron-donating substituents (e.g., $^{-}OCH_3$ and $^{-}$OH) attached to methoxyphenols elevate the π-electron density of the aromatic ring, facilitating their aqueous-phase reactions (He et al., 2019; Li et al., 2021; Jain et al., 2026).

3.2 Aqueous-phase SOA formation

Earlier studies have reported that aqueous-phase reactions of representative methoxyphenols with $^{\bullet}$OH and $^{3}C^*$ produce substantial low-volatility products and possess high aqSOA mass yields (Huang et al., 2018; Ma et al., 2021; Smith et al., 2014, 2015; Ye et al., 2020; Yu et al., 2016). To clarify whether $SO_4^{\bullet-}$-initiated reactions of VAA, VAL, and CFA also produce considerable amounts of aqSOA, time-dependent variations in aqSOA mass yields were investigated in this work and shown in Fig. 2a. It is noticeable that VAA, VAL, and CFA had significant aqSOA formation potentials, and their corresponding aqSOA mass yields at 30 min were 66.41%, 70.49%, and

https://doi.org/10.5194/egusphere-2026-5353
Preprint. Discussion started: 29 September 2026

63.12%, respectively. As illustrated in Fig. S2, aqSOA mass yields for five methoxyphenols (i.e., vanillyl alcohol, guaiacyl acetone, ferulic acid, syringic acid, and syringyl acetone) upon reactions with $^{\bullet}OH$ range from approximately 67% to 90% (Ma et al., 2021). By contrast, their corresponding yields from reactions with $^{3}C^{*}$ vary between 59% and 99% (Arciva et al., 2022). In addition, the maximum aqSOA mass yields for 4-methylsyringol and eugenol in reactions with $^{\bullet}OH$ can exceed 150%, followed by significant declines as the reactions proceed (Ye et al., 2020). Overall, aqSOA mass yields obtained in this work are comparable to those for other methoxyphenols in aqueous-phase reactions with $^{\bullet}OH$ and $^{3}C^{*}$. Thus, aqueous-phase reactions between methoxyphenols and $SO_4^{\bullet-}$ constitute a non-negligible pathway for aqSOA formation and should deserve greater attention in future studies.

As shown in Fig. 2a, the rapid aqSOA formation observed in the aqueous-phase reactions of the three methoxyphenols can be reasonably attributed to the efficient generation of substantial low-volatility products, including functionalized derivatives and oligomers (Arciva et al., 2022; Huang et al., 2018; Smith et al., 2014; Yu et al., 2016). In addition, a pronounced decrease in aqSOA mass yields was observed as the reaction time extends to 180 min, with corresponding yields of 24.20% for VAA, 23.59% for VAL, and 19.11% for CFA. This can be explained by the fact that fragmentation processes dominated the reactions during this period, leading to the substantial formation of highly volatile fragmented products (Chen et al., 2020; Huang et al., 2018; Ye et al., 2020). Such species are difficult to retain in the particulate phase, making

https://doi.org/10.5194/egusphere-2026-5353
Preprint. Discussion started: 29 September 2026

them unfavorable for aqSOA formation and unable to be efficiently detected by the HR-ToF-AMS (Decarlo et al., 2006). Consistent trends have also been reported for aqueous-phase reactions of 4-methylsyringol and eugenol with $^{\bullet}OH$ and $^{3}C^{*}$ (Chen et al., 2020; Ye et al., 2020). In our recent study, mild declining trends in aqSOA mass yields were also observed for guaiacol and syringol upon reactions with $SO_4^{\bullet-}$ (Chen et al., 2026).

To further unravel variation trend of aqSOA composition along with aging process, time-dependent changes of element ratios (H/C and O/C) and fractions of organic ion groups including CH, CHO, and CHOgt1 (containing more than one oxygen atom) were investigated. Meanwhile, the average carbon oxidation state ($OS_C = 2O/C - H/C$) was calculated based on the element ratios of aqSOA determined by the HR-ToF-AMS. Compared with the single O/C ratio, OS_C is widely regarded as a more accurate indicator of the oxidation degree of atmospheric organic matters, because it accounts for the saturation state of carbon atoms in SOA constituents (Kroll et al., 2011). As shown in Figs. 2b and S3, the O/C ratios and OS_C values of aqSOA formed from the aqueous-phase reactions of the three methoxyphenols with $SO_4^{\bullet-}$ exhibited a gradual increasing trend, whereas the H/C ratios displayed an opposite trend as the reactions proceeded. Similar observations have been reported in earlier studies about aqueous-phase reactions of other five methoxyphenols (i.e., eugenol, 4-ethylguaiacol, 4-methylsyringol, syringaldehyde, and acetosyringone) with $^{\bullet}OH$ and $^{3}C^{*}$ (Chen et al., 2020; Huang et al., 2018; Ye et al., 2020). The maximum O/C ratios and OS_C values were within the ranges of 0.86-1.20 and 0.53-1.43, respectively, which fall within the

https://doi.org/10.5194/egusphere-2026-5353
Preprint. Discussion started: 29 September 2026

corresponding observed ranges for ambient low-volatility oxygenated organic aerosols (LV-OOA) (Ye et al., 2020; Kroll et al., 2011; Yu et al., 2016). The pronounced increases in O/C ratios and OS_C values indicate continuous oxidation of aqSOA constituents with the prolongation of reactions, along with the formation of more oxygen-containing functional groups in the products (Chen et al., 2020). The oxidation degree of aqSOA compositions were also well supported by the variations in mass spectra of aqSOA at different reaction time obtained by the HR-ToF-AMS. As shown in Fig. S4, the fractions of CH groups in aqSOA constituents decreased substantially for VAA, VAL, and CFA, falling from 35.2%, 63.0%, and 41.1% at 30 min to 15.8%, 36.0%, and 30.2% at 360 min, respectively. In contrast, significant increases were observed in the total fractions of CHO and CHOgt1 groups, rising from 64.8%, 37.0%, and 58.9% to 84.2%, 64.0%, and 69.8% for VAA, VAL, and CFA, respectively. In addition, we found that aqSOA mass yields declined with increasing OS_C values. This phenomenon is consistent with previous reports, which demonstrate that higher OS_C values correspond to more extensive aging of SOA (Ortega et al., 2016). Such aging process typically generates abundant highly volatile fragmented products via the C−C bond scission of low-generation products and thereby causes an overall reduction in SOA mass (Ortega et al., 2016; Ye et al., 2020; Huang et al., 2018).

The Van Krevelen (VK) triangle diagram of aqSOA is depicted in Fig. 2c, revealing that the H/C and O/C ratios of aqSOA constituents clustered within a narrow slope range from –1 to –0.5. This trend is consistent with previous observations for

https://doi.org/10.5194/egusphere-2026-5353
Preprint. Discussion started: 29 September 2026

atmospheric OA and aqueous-phase reactions of methoxyphenols with •OH (Heald et al., 2010; Huang et al., 2018; Chhabra et al., 2011). These results suggest carboxylic acid or equal amounts of hydroxy and carbonyl functional groups are generally added during the reaction process (Heald et al., 2010). Meanwhile, the data acquired after 120 min fall within the characteristic region of LV-OOA in VK-triangle diagram (Ng et al., 2011). Given that VAA, VAL, and CFA contain unsaturated carbon chains, the substantial loss of hydrogen suggests their extensive oxidation by $SO_4^{\bullet-}$. In general, aging trajectories shown in VK-triangle diagram are dependent on precursor species (e.g., VAL and isoprene) and its classes (e.g., biogenic and anthropogenic volatile organic compounds) (Chhabra et al., 2011).

3.3 Light-absorbing property

Biomass burning emissions are widely recognized as an important source of atmospheric brown carbon (BrC) (Li et al., 2023), which absorbs incoming solar shortwave radiation predominantly in the near-ultraviolet and short visible wavelengths, thereby perturbing Earth's radiative budget (Laskin et al., 2025). In this work, pronounced color changes were observed for the solution samples, all of which turned from transparent to brownish-yellow following the reactions, shown in Fig. S5. Therefore, time-series variations in UV-vis spectra of solution samples were analyzed. As shown in Fig. 3, CFA displayed a characteristic absorption peak at 340 nm. In contrast, VAA and VAL exhibited their characteristic peaks at 260 nm and 292 nm, and 280 nm and 308 nm, respectively. These absorptions are resulted from π–π* (> 180 nm)

https://doi.org/10.5194/egusphere-2026-5353
Preprint. Discussion started: 29 September 2026

and n–π* (270-350 nm) electronic transitions of benzene ring and its substituted groups (Li et al., 2021; Tang et al., 2020; Santos et al., 2016). The substitutes are either electron-withdrawing groups (i.e., C=C, −CHO, and −COOH) or electron-donating groups (i.e., −OH and $-OCH_3$) (Santos et al., 2016). The absorbance of the characteristic peaks for VAA and VAL first increased and then declined to nearly zero as the reaction proceeded up to 360 min. Similar trends have been documented in previous investigations regarding $^{\bullet}OH$-initiated aqueous oxidation of 4-methylsyringol and 2,4,6-trimethylphenol (Ye et al., 2020). This phenomenon can be interpreted as a combined effect between the degradation of parent compounds and the generation of complex products (e.g., oligomerized and functionalized species) (Ye et al., 2020). In contrast, the absorbance of CFA at 340 nm decreased steadily over the entire reaction period, with an obvious drop observed after 60 min. This behavior is likely attributable to the degradation of CFA by $SO_4^{\bullet-}$ (Ye et al., 2020).

As illustrated in Fig. 3, the overall spectral profiles of VAA, VAL, and CFA changed markedly over the corresponding reactions. Notably, absorbance rose within the near-ultraviolet and visible regions (320-420 nm), where the three methoxyphenols exhibited no light absorption. The results confirm the generation of new light-absorbing products. Similar redshifts in absorption peaks of VAA, VAL, and other methoxyphenols (e.g., syringic acid and guaiacol) have also been observed during their aqueous-phase reactions with $^{\bullet}OH$ (Li et al., 2021; Tang et al., 2020; Yang et al., 2023). Furthermore, the spectral profiles obtained in this work are consistent with those of

https://doi.org/10.5194/egusphere-2026-5353
Preprint. Discussion started: 29 September 2026

atmospheric HULIS (Baduel et al., 2010; Fan et al., 2016). Therefore, aqueous-phase reactions of methoxyphenols with $SO_4^{\bullet-}$ serve as a potential source of HULIS in atmospheric aqueous environments. The strong absorbance of HULIS at longer wavelengths mainly originates from highly condensed, high-molecular-weight aromatic structures (Chen et al., 2002). In addition, all absorbance at longer wavelengths (320 nm for VAA, 356 nm for VAL, and 410 nm for CFA) initially increased and subsequently declined over the course of the reactions. Concurrently, the color of the reaction solutions gradually lightened over time. The observations indicate that novel chromophores were first formed and gradually degraded in the ensuing reactions (Li et al., 2021; Saleh et al., 2013; Santos et al., 2016; Tang et al., 2020; Wong et al., 2017; Zhao et al., 2015). Analogous trends have been reported for the aqueous-phase reactions of VAA, VAL, and syringic acid with $^{\bullet}OH$ (Li et al., 2021; Santos et al., 2016; Tang et al., 2020), as well as guaiacol and syringol with $SO_4^{\bullet-}$ (Chen et al., 2026). Additionally, this evolutionary trend resembles the photochemical aging process of BrC emitted from biomass burning (Saleh et al., 2013; Wong et al., 2017; Zhao et al., 2015).

To further characterize the fluorescence property of solution samples, fluorescence spectroscopy was employed herein, owing to its excellent performance in identifying atmospheric HULIS (Fan et al., 2016). As shown in Fig. S6, the initial EEM spectra of VAA, VAL, and CFA solutions exhibited characteristic fluorescence bands centered at Ex/Em = (200–300)/(300–400) nm, Ex/Em = (200–350)/(320–480) nm, and Ex/Em = (250–300)/(350–450) nm, respectively. Such features align with the representative

https://doi.org/10.5194/egusphere-2026-5353
Preprint. Discussion started: 29 September 2026

fluorescence characteristics of HULIS in smoke particles (Fan et al., 2016). Following reactions, the fluorescence bands of the three methoxyphenols redshifted. New distinct fluorescence bands for VAA, VAL, and CFA emerged at Ex/Em = (250–400)/(300–500) nm, (250–350)/(320–520) nm, and (280–380)/(380–500) nm, respectively. Such redshifts in fluorescence bands are generally linked to the generation of more complex products featuring greater conjugation (Chang and Thompson, 2010). Compared with the fluorescence regions identified in biomass-burning smoke $PM_{2.5}$, the post-reaction fluorescence peaks measured in this work fall within the typical HULIS region (C peak) (Fan et al., 2016; Tang et al., 2020). Furthermore, Chen et al. (2016, 2019) have reported that atmospheric organic aerosol-associated HULIS exhibit characteristic fluorescence emission spanning from 400 nm to 500 nm.

Ng et al. (2010) have reported that the mass spectral signatures of atmospheric LV-OOA closely resemble those of HULIS, because highly oxidized LV-OOA comprises polycarboxylic acids or acid-derived structures analogous to HULIS. Given the above-mentioned oxidation degree of aqSOA as well as the VK-triangle diagram results, aqSOA formed from the three methoxyphenols in this work can be classified as LV-OOA. In AMS mass spectra, the dominant fragment ions for HULIS are m/z = 44, along with other minor fragments (e.g., m/z = 29 and 40) (Paglione et al., 2014; Hawkins et al., 2016). Accordingly, time series profiles of the organic mass fractions of m/z = 44 (f_{44}) and m/z = 29 (f_{29}) are presented in Fig. S7. The gradual increases in both f_{44} and f_{29} suggest that progressive accumulation of HULIS-like components within the

https://doi.org/10.5194/egusphere-2026-5353
Preprint. Discussion started: 29 September 2026

products as the reactions progressed. This observation is well supported by the time-dependent trends in HULIS concentrations (Fig. S8). HULIS concentrations increased gradually and reached 17.91 mg L^{-1} for VAA, 18.67 mg L^{-1} for VAL, and 25.78 mg L^{-1} for CFA at 240 min, respectively, before remaining relatively stable for the subsequent reaction period. In this work, the HULIS fraction isolated via polymer-based solid-phase extraction is primarily composed of low-molecular-weight organic acids, fulvic acids, and other humic substances (Li et al., 2022). According to the above observations and discussion, the aqueous-phase reactions of the three methoxyphenols with $SO_4^{\bullet-}$ are a potential source of HULIS in atmospheric aqueous environments.

3.4 Oxidation potential

Oxidation potential describes the capacity of substances to generate reactive oxygen species (ROS) or deplete antioxidants, and is widely adopted as a metric to assess biological oxidative stress (Bates et al., 2019). In general, DTT assay is commonly used to characterize the oxidation potential level of reaction products, because its consumed amounts are directly proportional to the quantity of redox-active substances (Jiang et al., 2019). As shown in Fig. 4a, the DTT consumed mass (M_{DTT}) of VAA, VAL, CFA, and blank samples exhibited linear correlations with incubation time ($R^2 > 0.95$). The corresponding consumption rates (R_{DTT}) represent the oxidation potential, which were 0.069 μM min^{-1} for VAA, 0.073 μM min^{-1} for VAL, 0.079 μM min^{-1} for CFA, and 0.041 μM min^{-1} for blank sample, respectively. The observed M_{DTT} value of blank sample was likely due to dissolved oxygen in deionized water (Li et al.,

https://doi.org/10.5194/egusphere-2026-5353
Preprint. Discussion started: 29 September 2026

2022). The differences in R_{DTT} values of the three methoxyphenols shown in Fig. 4a are attributed from the distinct substituents on the 2-methoxyphenol backbone. As described in Section 3.1, CFA is more susceptible to oxidation than VAA and VAL, which accounts for its higher R_{DTT} value. This trend is consistent with their second-order rate constants. As illustrated in Fig. 4b, the DTT activity of the three methoxyphenols followed a similar trend, which rose rapidly at the initial stage of the reactions and then gradually declined as the reactions proceeded. Overall, the DTT activity measured over the course of reactions is higher than that of parent compounds. The findings indicate that oxidation products generated from aqueous-phase reactions of methoxyphenols with $SO_4^{\bullet-}$ possessed higher oxidation potentials, which posed greater health risks than their precursors (Bates et al., 2019; Jiang et al., 2019). Comparable trends have been reported for eugenol undergoing aqueous-phase reactions with $^{\bullet}OH$ and $^3C^*$ (Li et al., 2022). The enhanced oxidation potential of reaction products is a widely-documented phenomenon associated with atmospheric aging processes (Lei et al., 2023; Bates et al., 2019). As illustrated in Figs. 2b and 4b, higher O/C ratios and OS_C values did not correspond to higher R_{DTT} values, underscoring that precursor identity governs the oxidation potential of aqSOA (Tuet et al., 2017). This observation holds for both laboratory-generated SOA and ambient atmospheric OA (Tuet et al., 2017; Xu et al., 2015a; Xu et al., 2015b; Verma et al., 2015). In general, R_{DTT} reaches a peak when highly reactive oxidation products accumulate via functionalization during the initial aging stage, and subsequently declines owing to the

https://doi.org/10.5194/egusphere-2026-5353
Preprint. Discussion started: 29 September 2026

evaporation of smaller, higher-volatility redox-active molecules generated from fragmentation (Wang et al., 2018).

4 Conclusions and atmospheric implications

This work provides updated kinetic data for aqueous-phase reactions of three representative substituted methoxyphenols with $SO_4^{\bullet-}$, and further elucidates aqSOA mass yields, optical properties, and oxidation potentials. The kinetic data have important implications for the fate of methoxyphenols in atmospheric aqueous environments. The atmospheric lifetimes of VAA, VAL, and CFA were in the ranges of 0.32-50.54 h, 0.30-47.22 h, and 0.23-35.94 h, respectively, calculated according to the $k_{2,M}$ values obtained in this work and a typically average $SO_4^{\bullet-}$ concentration ranging from 3.6×10^{-13} to 2.3×10^{-15} mol L^{-1} in atmospheric cloud droplets and deliquescent particles (Herrmann et al., 2010). Their lifetimes may be further shortened when other aqueous-phase degradation pathways (e.g., reactions with $^{\bullet}OH$ and $^3C^*$) are taken into account. Given that the obtained second-order rate constants were comparable to those reported for other methoxyphenols reacting with $^{\bullet}OH$ and $^3C^*$, $SO_4^{\bullet-}$-initiated degradation reasonably represents a vital transformation pathway of substituted methoxyphenols in atmospheric aqueous environments.

Significant aqSOA mass yields and its light-absorbing property observed in this work suggest that $SO_4^{\bullet-}$-initiated aqueous-phase reactions of substituted methoxyphenols are a potential pathway for formation of aqSOA and HULIS in atmospheric aqueous environments. Recent field observations have suggested that

https://doi.org/10.5194/egusphere-2026-5353
Preprint. Discussion started: 29 September 2026

aqSOA formed from biomass burning emissions contributes substantially to haze pollution in China (Xiao et al., 2022; Xue et al., 2025). Notably, methoxyphenols account for up to 80% of the total mass of aqSOA generated from phenolic precursors (Xiao et al., 2022). Given that the concentration of phenols and substituted phenols can exceed 100 μM in fog waters impacted by biomass burning (Yu et al., 2016). the mass concentration of aqSOA produced via aqueous-phase reactions of phenolic species with $SO_4^{\bullet-}$ can be crudely estimated to approximately 6 mg L^{-1}. This calculation adopts the minimum aqSOA mass yield (63.12%) at 30 min determined in this work and the lowest molecular weight among phenolic compounds (MW = 98). Therefore, more attention should be paid to aqSOA formation in regions impacted by biomass burning and wildfires. In addition, the oxidation potentials of oxidation products for all three methoxyphenols were higher than those of parent compounds. This indicates that products generated during $SO_4^{\bullet-}$-initiated oxidation of methoxyphenols posed a relatively high potential risk of oxidative stress to human health (Bates et al., 2019; Lei et al., 2023). Considering that the DTT assay alone cannot fully evaluate the toxicity of complex atmospheric mixtures, future studies should incorporate multiple biological indicators to achieve a more comprehensive toxicological assessment. Overall, aqueous-phase reactions of substituted methoxyphenols with $SO_4^{\bullet-}$ substantially modulate the physicochemical properties of atmospheric particles, especially in regions impacted by biomass burning. In addition, incorporating the kinetic parameters and aqSOA mass yields into current atmospheric models would help improve the predictive

https://doi.org/10.5194/egusphere-2026-5353
Preprint. Discussion started: 29 September 2026

performance of model simulations.

Data availability. The experimental data are available upon request to the corresponding authors.

Supplement. The supplement related to this article is available.

Author contributions. R.C., T.C., and C.L. conceived the study, R.C. and X.L. performed the experiments and conducted the data analyses. R.C., X.L., X.H., and R.L. interpreted and discussed the data results. R.C., T.C., and C.L. wrote and revised the manuscript. All coauthors contributed to discussions and suggestions in finalizing the manuscript.

Competing interests. The contact author has declared that none of the authors has any competing interests.

Acknowledgements. This work was financially supported by the Jing-Jin-Ji Regional Integrated Environmental Improvement-National Science and Technology Major Project (2026ZD1209500) and the Scientific Research Foundation for Advanced Talents of Sichuan Normal University (XJ20240042).

References

An, Z., Sun, J., Han, D., Mei, Q., Wei, B., Wang, X., Xie, J., Zhan, J., and He, M.: Effect of pH on ·OH-induced degradation progress of syringol/syringaldehyde and health effect, Chemosphere, 255, 126893, https://doi.org/10.1016/j.chemosphere.2020.126893, 2020.

Arciva, S., Niedek, C., Mavis, C., Yoon, M., Sanchez, M. E., Zhang, Q., and Anastasio,

https://doi.org/10.5194/egusphere-2026-5353
Preprint. Discussion started: 29 September 2026

C.: Aqueous ·OH oxidation of highly substituted phenols as a source of secondary organic aerosol, Environ. Sci. Technol., 56, 9959-9967, https://doi.org/10.1021/acs.est.2c02225, 2022.

Baduel, C., Voisin, D., and Jaffrezo, J. L.: Seasonal variations of concentrations and optical properties of water soluble HULIS collected in urban environments, Atmos. Chem. Phys., 10, 4085-4095, https://doi.org/10.5194/acp-10-4085-2010, 2010.

Bates, J. T., Fang, T., Verma, V., Zeng, L., Weber, R. J., Tolbert, P. E., Abrams, J. Y., Sarnat, S. E., Klein, M., Mulholland, J. A., and Russell, A. G.: Review of acellular assays of ambient particulate matter oxidative potential: methods and relationships with composition, sources, and health effects, Environ. Sci. Technol., 53, 4003-4019, https://doi.org/10.1021/acs.est.8b03430, 2019.

Chang, J. L. and Thompson, J. E.: Characterization of colored products formed during irradiation of aqueous solutions containing H_2O_2 and phenolic compounds, Atmos. Environ., 44, 541-551, https://doi.org/10.1016/j.atmosenv.2009.10.042, 2010.

Chataigner, I., Panel, C., Gérard, H., and Piettre, S. R.: Sulfonyl vs. carbonyl group: which is the more electron-withdrawing?, Chem. Commun., 43, 3288-3290, https://doi.org/10.1039/b705034h, 2007.

Chen, J., Gu, B., LeBoeuf, E. J., Pan, H., and Dai, S.: Spectroscopic characterization of the structural and functional properties of natural organic matter fractions, Chemosphere, 48, 59-68, https://doi.org/10.1016/S0045-6535(02)00041-3, 2002.

Chen, Q., Ikemori, F., and Mochida, M.: Light absorption and excitation–emission

https://doi.org/10.5194/egusphere-2026-5353
Preprint. Discussion started: 29 September 2026

480 fluorescence of urban organic aerosol components and their relationship to
481 chemical structure, Environ. Sci. Technol., 50, 10859-10868,
482 https://doi.org/10.1021/acs.est.6b02541, 2016.
483 Chen, Q., Wang, M., Wang, Y., Zhang, L., Li, Y., and Han, Y.: Oxidative potential of
484 water-soluble matter associated with chromophoric substances in $PM_{2.5}$ over Xi'an,
485 China, Environ. Sci. Technol., 53, 8574-8584,
486 https://doi.org/10.1021/acs.est.9b01976, 2019.
487 Chen, R., Li, X., Zhou, X., Chen, T., Yang, Z., Fan, L., Sun, M., Niu, Q., Liu, C., and
488 He, H.: Sulfate radical-initiated aqueous oxidation of biomass burning tracers: a
489 potential source of HULIS and aqSOA, Environ. Sci. Technol., 60, 9381-9391,
490 https://doi.org/10.1021/acs.est.5c14755, 2026.
491 Chen, Y., Li, N., Li, X., Tao, Y., Luo, S., Zhao, Z., Ma, S., Huang, H., Chen, Y., Ye, Z.,
492 and Ge, X.: Secondary organic aerosol formation from $^3C^*$-initiated oxidation of
493 4-ethylguaiacol in atmospheric aqueous-phase, Sci. Total Environ., 723, 137953,
494 https://doi.org/10.1016/j.scitotenv.2020.137953, 2020.
495 Chhabra, P. S., Ng, N. L., Canagaratna, M. R., Corrigan, A. L., Russell, L. M., Worsnop,
496 D. R., Flagan, R. C., and Seinfeld, J. H.: Elemental composition and oxidation of
497 chamber organic aerosol, Atmos. Chem. Phys., 11, 8827-8845,
498 https://doi.org/10.5194/acp-11-8827-2011, 2011.
499 Cope, J. D., Bates, K. H., Tran, L. N., Abellar, K. A., and Nguyen, T. B.: Sulfur radical
500 formation from the tropospheric irradiation of aqueous sulfate aerosols, Proc. Nat.

https://doi.org/10.5194/egusphere-2026-5353
Preprint. Discussion started: 29 September 2026

Acad. Sci. USA, 119, e2202857119, https://doi.org/10.1073/pnas.2202857119, 2022.

DeCarlo, P. F., Kimmel, J. R., Trimborn, A., Northway, M. J., Jayne, J. T., Aiken, A. C., Gonin, M., Fuhrer, K., Horvath, T., Docherty, K. S., Worsnop, D. R., and Jimenez, J. L.: Field-deployable, high-resolution, time-of-flight aerosol mass spectrometer, Anal. Chem., 78, 8281-8289, https://doi.org/10.1021/ac061249n, 2006.

Fan, X., Wei, S., Zhu, M., Song, J., and Peng, P.: Comprehensive characterization of humic-like substances in smoke $PM_{2.5}$ emitted from the combustion of biomass materials and fossil fuels, Atmos. Chem. Phys., 16, 13321-13340, https://doi.org/10.5194/acp-16-13321-2016, 2016.

Gould, E. S.: Mechanism and Structure in Organic Chemistry, New York: Holt, Rinehart and Winston, 1959.

Hawkins, L. N., Lemire, A. N., Galloway, M. M., Corrigan, A. L., Turley, J. J., Espelien, B. M., and De Haan, D. O.: Maillard chemistry in clouds and aqueous aerosol as a source of atmospheric humic-like substances, Environ. Sci. Technol., 50, 7443-7452, https://doi.org/10.1021/acs.est.6b00909, 2016.

He, L., Schaefer, T., Otto, T., Kroflič, A., and Herrmann, H.: Kinetic and theoretical study of the atmospheric aqueous-phase reactions of OH radicals with methoxyphenolic compounds, J. Phys. Chem. A, 123, 7828-7838, https://doi.org/10.1021/acs.jpca.9b05696, 2019.

Heald, C. L., Kroll, J. H., Jimenez, J. L., Docherty, K. S., DeCarlo, P. F., Aiken, A. C.,

https://doi.org/10.5194/egusphere-2026-5353
Preprint. Discussion started: 29 September 2026

Chen, Q., Martin, S. T., Farmer, D. K., and Artaxo, P.: A simplified description of the evolution of organic aerosol composition in the atmosphere, Geophys. Res. Lett., 37, https://doi.org/10.1029/2010GL042737, 2010.

Herrmann, H., Hoffmann, D., Schaefer, T., Bräuer, P., and Tilgner, A.: Tropospheric aqueous-phase free-radical chemistry: radical sources, spectra, reaction kinetics and prediction tools, ChemPhysChem, 11, 3796-3822, https://doi.org/10.1002/cphc.201000533, 2010.

Herrmann, H., Schaefer, T., Tilgner, A., Styler, S. A., Weller, C., Teich, M., and Otto, T.: Tropospheric aqueous-phase chemistry: kinetics, mechanisms, and its coupling to a changing gas phase, Chem. Rev., 115, 4259-4334, https://doi.org/10.1021/cr500447k, 2015.

Huang, D. D., Zhang, Q., Cheung, H. H. Y., Yu, L., Zhou, S., Anastasio, C., Smith, J. D., and Chan, C. K.: Formation and evolution of aqSOA from aqueous-phase reactions of phenolic carbonyls: comparison between ammonium sulfate and ammonium nitrate slutions, Environ. Sci. Technol., 52, 9215-9224, https://doi.org/10.1021/acs.est.8b03441, 2018.

Jaffé, H. H.: A reëxamination of the Hammett equation, Chem. Rev., 53, 191-261, https://doi.org/10.1021/cr60165a003, 2002.

Jain, P., Witkowski, B., Szlęk, J., and Gierczak, T.: Aqueous OH kinetics of aliphatic carboxylic acids: new data and updated structure–activity relationship, J. Phys. Chem. A, 130, 2853 - 2870, https://doi.org/10.1021/acs.jpca.5c06518, 2026.

https://doi.org/10.5194/egusphere-2026-5353
Preprint. Discussion started: 29 September 2026

543 Jiang, H., Liu, Y., Xie, Y., Liu, J., Chen, T., Ma, Q., and He, H.: Oxidation potential
544 reduction of carbon nanomaterials during atmospheric-relevant aging: role of
545 surface coating, Environ. Sci. Technol., 53, 10454-10461,
546 https://doi.org/10.1021/acs.est.9b02062, 2019.
547 Kaur, R. and Anastasio, C.: First measurements of organic triplet excited states in
548 atmospheric waters, E Environ. Sci. Technol., 52, 5218-5226,
549 https://doi.org/10.1021/acs.est.7b06699, 2018.
550 Kitanovski, Z., Čusak, A., Grgić, I., and Claeys, M.: Chemical characterization of the
551 main products formed through aqueous-phase photonitration of guaiacol, Atmos.
552 Meas. Tech., 7, 2457-2470, https://doi.org/10.5194/amt-7-2457-2014, 2014.
553 Kroll, J. H., Donahue, N. M., Jimenez, J. L., Kessler, S. H., Canagaratna, M. R., Wilson,
554 K. R., Altieri, K. E., Mazzoleni, L. R., Wozniak, A. S., Bluhm, H., Mysak, E. R.,
555 Smith, J. D., Kolb, C. E., and Worsnop, D. R.: Carbon oxidation state as a metric
556 for describing the chemistry of atmospheric organic aerosol, Nat. Chem., 3, 133-
557 139, https://doi.org/10.1038/nchem.948, 2011.
558 Kwong, K. C., Chim, M. M., Davies, J. F., Wilson, K. R., and Chan, M. N.: Importance
559 of sulfate radical anion formation and chemistry in heterogeneous OH oxidation
560 of sodium methyl sulfate, the smallest organosulfate, Atmos. Chem. Phys., 18,
561 2809-2820, https://doi.org/10.5194/acp-18-2809-2018, 2018.
562 Lai, R. W. S., Qiu, T., Zhang, X., Wang, Y., Hao, T., Ge, X., Du, L., Tang, M., Hoi, K.
563 I., Mok, K. M., and Li, Y. J.: Deciphering the key drivers of oxidative potential

https://doi.org/10.5194/egusphere-2026-5353
Preprint. Discussion started: 29 September 2026

564 during ammonium nitrate-mediated aqueous-phase photoreaction of
565 methoxyphenols, Atmos. Environ., 340, 120895,
566 https://doi.org/10.1016/j.atmosenv.2024.120895, 2025.
567 Laskin, A., West, C. P., and Hettiyadura, A. P. S.: Molecular insights into the
568 composition, sources, and aging of atmospheric brown carbon, Chem. Soc. Rev.,
569 54, X 2025-2002-2008, https://doi.org/10.1039/d3cs00609c, 2025.
570 Lei, R., Wei, Z., Chen, M., Meng, H., Wu, Y., and Ge, X.: Aging effects on the toxicity
571 alteration of different types of organic aerosols: a review, Curr. Pollut. Rep., 9,
572 590-601, https://doi.org/10.1007/s40726-023-00272-9, 2023.
573 Li, F., Tsona, N. T., Li, J., and Du, L.: Aqueous-phase oxidation of syringic acid emitted
574 from biomass burning: formation of light-absorbing compounds, Sci. Total
575 Environ., 765, 144239, https://doi.org/10.1016/j.scitotenv.2020.144239, 2021.
576 Li, F., Zhou, S., Du, L., Zhao, J., Hang, J., and Wang, X.: Aqueous-phase chemistry of
577 atmospheric phenolic compounds: a critical review of laboratory studies, Sci. Total
578 Environ., 856, 158895, https://doi.org/10.1016/j.scitotenv.2022.158895, 2023.
579 Li, X., Tao, Y., Zhu, L., Ma, S., Luo, S., Zhao, Z., Sun, N., Ge, X., and Ye, Z.: Optical
580 and chemical properties and oxidative potential of aqueous-phase products from
581 OH and $^{3}C^{*}$-initiated photooxidation of eugenol, Atmos. Chem. Phys., 22, 7793-
582 7814, https://doi.org/10.5194/acp-22-7793-2022, 2022.
583 Liu, C., Chen, D., and Chen, X. e.: Atmospheric reactivity of methoxyphenols: a review,
584 Environ. Sci. Technol., 56, 2897-2916, https://doi.org/10.1021/acs.est.1c06535,

https://doi.org/10.5194/egusphere-2026-5353
Preprint. Discussion started: 29 September 2026

2022.

Liu, C., Wu, B., and Chen, X. e.: Sulfate radical-based oxidation for sludge treatment: a review, Chem. Eng. J., 335, 865-875, https://doi.org/10.1016/j.cej.2017.10.162, 2018.

Loisel, G., Mekic, M., Liu, S., Song, W., Jiang, B., Wang, Y., Deng, H., and Gligorovski, S.: Ionic strength effect on the formation of organonitrate compounds through photochemical degradation of vanillin in liquid water of aerosols, Atmos. Environ., 246, 118140, https://doi.org/10.1016/j.atmosenv.2020.118140, 2021.

Luo, S., Wei, Z., Dionysiou, D. D., Spinney, R., Hu, W.-P., Chai, L., Yang, Z., Ye, T., and Xiao, R.: Mechanistic insight into reactivity of sulfate radical with aromatic contaminants through single-electron transfer pathway, Chem. Eng. J., 327, 1056-1065, https://doi.org/10.1016/j.cej.2017.06.179, 2017.

Ma, L., Guzman, C., Niedek, C., Tran, T., Zhang, Q., and Anastasio, C.: Kinetics and mass yields of aqueous secondary organic aerosol from highly substituted phenols reacting with a triplet excited state, Environ. Sci. Technol., 55, 5772-5781, https://doi.org/10.1021/acs.est.1c00575, 2021.

McFall, A. S., Johnson, A. W., and Anastasio, C.: Air–water partitioning of biomass-burning phenols and the effects of temperature and salinity, Environ. Sci. Technol., 54, 3823-3830, https://doi.org/10.1021/acs.est.9b06443, 2020.

Neta, P., Huie, R. E., and Ross, A. B.: Rate constants for reactions of inorganic radicals in aqueous solution, J. Phys. Chem. Ref. Data, 17, 1027-1284,

https://doi.org/10.5194/egusphere-2026-5353
Preprint. Discussion started: 29 September 2026

606 https://doi.org/10.1063/1.555808, 1988.

607 Ng, N. L., Canagaratna, M. R., Jimenez, J. L., Chhabra, P. S., Seinfeld, J. H., and
608 Worsnop, D. R.: Changes in organic aerosol composition with aging inferred from
609 aerosol mass spectra, Atmos. Chem. Phys., 11, 6465-6474,
610 https://doi.org/10.5194/acp-11-6465-2011, 2011.

611 Ng, N. L., Canagaratna, M. R., Zhang, Q., Jimenez, J. L., Tian, J., Ulbrich, I. M., Kroll,
612 J. H., Docherty, K. S., Chhabra, P. S., Bahreini, R., Murphy, S. M., Seinfeld, J. H.,
613 Hildebrandt, L., Donahue, N. M., DeCarlo, P. F., Lanz, V. A., Prévôt, A. S. H.,
614 Dinar, E., Rudich, Y., and Worsnop, D. R.: Organic aerosol components observed
615 in Northern Hemispheric datasets from Aerosol Mass Spectrometry, Atmos. Chem.
616 Phys., 10, 4625-4641, https://doi.org/10.5194/acp-10-4625-2010, 2010.

617 Nolte, C. G., Schauer, J. J., Cass, G. R., and Simoneit, B. R. T.: Highly polar organic
618 compounds present in wood smoke and in the ambient atmosphere, Environ. Sci.
619 Technol., 35, 1912-1919, https://doi.org/10.1021/es001420r, 2001.

620 O'Neill, P. and Steenken, S.: Pulse radiolysis and electron spin resonance studies on the
621 formation of phenoxyl radicals by reaction of OH radicals with methoxylated
622 phenols and hydroxybenzoic acids, Ber. Bunsenges. Phys. Chem., 81, 550-556,
623 https://doi.org/10.1002/bbpc.19770810603, 1977.

624 Ortega, A. M., Hayes, P. L., Peng, Z., Palm, B. B., Hu, W., Day, D. A., Li, R., Cubison,
625 M. J., Brune, W. H., Graus, M., Warneke, C., Gilman, J. B., Kuster, W. C., de Gouw,
626 J., Gutiérrez-Montes, C., and Jimenez, J. L.: Real-time measurements of secondary

https://doi.org/10.5194/egusphere-2026-5353
Preprint. Discussion started: 29 September 2026

organic aerosol formation and aging from ambient air in an oxidation flow reactor in the Los Angeles area, Atmos. Chem. Phys., 16, 7411-7433, https://doi.org/10.5194/acp-16-7411-2016, 2016.

Paglione, M., Kiendler-Scharr, A., Mensah, A. A., Finessi, E., Giulianelli, L., Sandrini, S., Facchini, M. C., Fuzzi, S., Schlag, P., Piazzalunga, A., Tagliavini, E., Henzing, J. S., and Decesari, S.: Identification of humic-like substances (HULIS) in oxygenated organic aerosols using NMR and AMS factor analyses and liquid chromatographic techniques, Atmos. Chem. Phys., 14, 25-45, https://doi.org/10.5194/acp-14-25-2014, 2014.

Pan, M., Chen, Z., Shan, C., Wang, Y., Pan, B., and Gao, G.: Photochemical activation of seemingly inert SO_4^{2-} in specific water environments, Chemosphere, 214, 399-407, https://doi.org/10.1016/j.chemosphere.2018.09.123, 2019.

Pang, H., Zhang, Q., Lu, X., Li, K., Chen, H., Chen, J., Yang, X., Ma, Y., Ma, J., and Huang, C.: Nitrite-mediated photooxidation of vanillin in the atmospheric aqueous phase. Environ. Sci. Technol., 53, 14253-14263, https://doi.org/10.1021/acs.est.9b03649, 2019.

Paul, J., Jensen, S., Dukart, A., and Cornelissen, G.: Optimization of a preparative multimodal ion exchange step for purification of a potential malaria vaccine, J. Chromatogr. A, 1366, 38-44, https://doi.org/10.1016/j.chroma.2014.09.029, 2014.

Rudziński, K. J. and Szmigielski, R.: Aqueous reactions of sulfate radical-anions with nitrophenols in atmospheric context, Atmosphere, 10, 795,

https://doi.org/10.5194/egusphere-2026-5353
Preprint. Discussion started: 29 September 2026

https://doi.org/10.3390/atmos10120795, 2019.

Saleh, R., Hennigan, C. J., McMeeking, G. R., Chuang, W. K., Robinson, E. S., Coe, H., Donahue, N. M., and Robinson, A. L.: Absorptivity of brown carbon in fresh and photo-chemically aged biomass-burning emissions, Atmos. Chem. Phys., 13, 7683-7693, https://doi.org/10.5194/acp-13-7683-2013, 2013.

Santos, G. T. A. D., Santos, P. S. M., and Duarte, A. C.: V anillic and syringic acids from biomass burning: behaviour during Fenton-like oxidation in atmospheric aqueous phase and in the absence of light, J. Hazard. Mater., 313, 201-208, https://doi.org/10.1016/j.jhazmat.2016.04.006, 2016.

Smith, J. D., Kinney, H., and Anastasio, C.: Aqueous benzene-diols react with an organic triplet excited state and hydroxyl radical to form secondary organic aerosol, Phys. Chem. Chem. Phys., 17, 10227-10237, https://doi.org/10.1039/c4cp06095d, 2015.

Smith, J. D., Sio, V., Yu, L., Zhang, Q., and Anastasio, C.: Secondary organic aerosol production from aqueous reactions of atmospheric phenols with an organic triplet excited state, Environ. Sci. Technol., 48, 1049-1057, https://doi.org/10.1021/es4045715, 2014.

Tang, S., Li, F., Tsona, N. T., Lu, C., Wang, X., and Du, L.: Aqueous-phase photooxidation of vanillic acid: a potential source of humic-like substances (HULIS), ACS Earth Space Chem., 4, 862-872, https://doi.org/10.1021/acsearthspacechem.0c00070, 2020.

https://doi.org/10.5194/egusphere-2026-5353
Preprint. Discussion started: 29 September 2026

669 Tong, X., Wang, S., and Wang, L.: Kinetics and mechanism of syringic acid degradation
670 initiated by hydroxyl radical and sulphate radical in the aqueous phase,
671 Chemosphere, 256, 126997, https://doi.org/10.1016/j.chemosphere.2020.126997,
672 2020.
673 Tuet, W. Y., Chen, Y., Xu, L., Fok, S., Gao, D., Weber, R. J., and Ng, N. L.: Chemical
674 oxidative potential of secondary organic aerosol (SOA) generated from the
675 photooxidation of biogenic and anthropogenic volatile organic compounds, Atmos.
676 Chem. Phys., 17, 839-853, https://doi.org/10.5194/acp-17-839-2017, 2017.
677 Verma, V., Fang, T., Xu, L., Peltier, R. E., Russell, A. G., Ng, N. L., and Weber, R. J.:
678 Organic aerosols associated with the generation of reactive oxygen species (ROS)
679 by water-soluble $PM_{2.5}$, Environ. Sci. Technol., 49, 4646-4656,
680 https://doi.org/10.1021/es505577w, 2015.
681 Wang, S., Ye, J., Soong, R., Wu, B., Yu, L., Simpson, A. J., and Chan, A. W. H.:
682 Relationship between chemical composition and oxidative potential of secondary
683 organic aerosol from polycyclic aromatic hydrocarbons, Atmos. Chem. Phys., 18,
684 3987-4003, https://doi.org/10.5194/acp-18-3987-2018, 2018.
685 Wojnárovits, L. and Takács, E.: Rate constants of sulfate radical anion reactions with
686 organic molecules: a review, Chemosphere, 220, 1014-1032,
687 https://doi.org/10.1016/j.chemosphere.2018.12.156, 2019.
688 Wong, J. P. S., Nenes, A., and Weber, R. J.: Changes in light absorptivity of molecular
689 weight separated brown carbon due to photolytic aging, Environ. Sci. Technol., 51,

https://doi.org/10.5194/egusphere-2026-5353
Preprint. Discussion started: 29 September 2026

690 8414-8421, https://doi.org/10.1021/acs.est.7b01739, 2017.
691 Xiao, Y., Hu, M., Li, X., Zong, T., Xu, N., Hu, S., Zeng, L., Chen, S., Song, Y., Guo, S.,
692 and Wu, Z.: Aqueous secondary organic aerosol formation attributed to phenols
693 from biomass burning, Sci. Total Environ., 847, 157582,
694 https://doi.org/10.1016/j.scitotenv.2022.157582, 2022.
695 Xu, L., Suresh, S., Guo, H., Weber, R. J., and Ng, N. L.: Aerosol characterization over
696 the southeastern United States using high-resolution aerosol mass spectrometry:
697 spatial and seasonal variation of aerosol composition and sources with a focus on
698 organic nitrates, Atmos. Chem. Phys., 15, 7307-7336, https://doi.org/10.5194/acp-
699 15-7307-2015, 2015a.
700 Xu, L., Guo, H., Boyd, C. M., Klein, M., Bougiatioti, A., Cerully, K. M., Hite, J. R.,
701 Isaacman-VanWertz, G., Kreisberg, N. M., Knote, C., Olson, K., Koss, A.,
702 Goldstein, A. H., Hering, S. V., de Gouw, J., Baumann, K., Lee, S.-H., Nenes, A.,
703 Weber, R. J., and Ng, N. L.: Effects of anthropogenic emissions on aerosol
704 formation from isoprene and monoterpenes in the southeastern United States, Proc.
705 Nat. Acad. Sci. USA, 112, 37-42, https://doi.org/10.1073/pnas.1417609112,
706 2015b.
707 Xue, S., Luo, H., Wang, Z., Shen, H., Zhang, Y., Nie, C., Song, Z., Wang, L., Wang, S.,
708 Chen, J., and Zhao, D.: Online molecular insights into sources and formation of
709 organic aerosol in Shanghai, npj Clim. Atmos. Sci., 8, 358,
710 https://doi.org/10.1038/s41612-025-01230-6, 2025.

https://doi.org/10.5194/egusphere-2026-5353
Preprint. Discussion started: 29 September 2026

711 Yang, J., Zhou, T., Lyu, Y., Go, B. R., Lam, J. C.-H., Chan, C. K., and Nah, T.: Effects
712 of copper on chemical kinetics and brown carbon formation in the aqueous ˙OH
713 oxidation of phenolic compounds, Environ. Sci. Proc. Imp., 26, 1526-1542,
714 https://doi.org/10.1039/D4EM00191E, 2024.
715 Yang, W., Ma, J., Nan, X., Yan, R., Tang, N., Du, T., and Han, C.: The pH dependence
716 of photochemical reactions between methoxyphenols with Fe(III)-oxalates, Atmos.
717 Environ., 303, 119749, https://doi.org/10.1016/j.atmosenv.2023.119749, 2023.
718 Ye, Z., Zhuang, Y., Chen, Y., Zhao, Z., Ma, S., Huang, H., Chen, Y., and Ge, X.:
719 Aqueous-phase oxidation of three phenolic compounds by hydroxyl radical:
720 insight into secondary organic aerosol formation yields, mechanisms, products and
721 optical properties, Atmos. Environ., 223, 117240,
722 https://doi.org/10.1016/j.atmosenv.2019.117240, 2020.
723 Yu, L., Smith, J., Laskin, A., George, K. M., Anastasio, C., Laskin, J., Dillner, A. M.,
724 and Zhang, Q.: Molecular transformations of phenolic SOA during photochemical
725 aging in the aqueous phase: competition among oligomerization, functionalization,
726 and fragmentation, Atmos. Chem. Phys., 16, 4511-4527,
727 https://doi.org/10.5194/acp-16-4511-2016, 2016.
728 Zhao, R., Lee, A. K. Y., Huang, L., Li, X., Yang, F., and Abbatt, J. P. D.: Photochemical
729 processing of aqueous atmospheric brown carbon, Atmos. Chem. Phys., 15, 6087-
730 6100, https://doi.org/10.5194/acp-15-6087-2015, 2015.
731 Zhu, H. P., Zhao, H. W., Zhang, Z. X., Wang, W. F., and Yao, S. D.: Laser flash

https://doi.org/10.5194/egusphere-2026-5353
Preprint. Discussion started: 29 September 2026

732 photolysis study on antioxidant properties of hydroxycinnamic acid derivatives,
733 Radiat. Environ. Biophys., 45, 73-77, https://doi.org/10.1007/s00411-006-0041-8,
734 2006.

https://doi.org/10.5194/egusphere-2026-5353
Preprint. Discussion started: 29 September 2026

735 **Table 1.** Second-order rate constants of VAA, VAL, and CFA in the aqueous-phase

736 reactions with $SO_4^{\bullet-}$.

methoxyphenols	structures	$k_{2,M}/k_{2,R}$	$k_{2,M}$ (10^9 M^{-1} s^{-1})	τ (h)[a]
vanillic acid (VAA, $C_8H_8O_4$, MW 168)	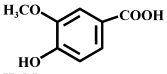	0.75 ± 0.06	2.40 ± 0.19	0.32-50.54
vanillin (VAL, $C_8H_8O_3$, MW 152)	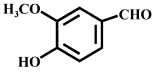	0.80 ± 0.03	2.56 ± 0.10	0.30-47.22
coniferyl aldehyde (CFA, $C_{10}H_{10}O_3$, MW 178)	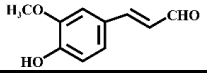	1.06 ± 0.08	3.37 ± 0.22	0.23-35.94

737 [a] Atmospheric lifetime (τ) is calculated using the equation $\tau=1/k_{2,M}[SO_4^{\bullet-}]$, where $[SO_4^{\bullet-}]$

738 is the average concentration of $SO_4^{\bullet-}$ in atmospheric aqueous environment, ranging

739 from 3.6×10^{-13} to 2.3×10^{-15} mol L^{-1} (Herrmann et al., 2010).

https://doi.org/10.5194/egusphere-2026-5353
Preprint. Discussion started: 29 September 2026

740 **Table 2.** Summary of second-order rate constants of methoxyphenols in the aqueous-

741 phase reactions with $SO_4^{\bullet-}$, $^{\bullet}OH$, and $^3C^*$.

oxidants	methoxyphenols	$k_{2,M}$ (M^{-1} s^{-1})	pH	τ (h)[a]	references
$SO_4^{\bullet-}$	VAA	$(2.40 \pm 0.19) \times 10^9$	2	4.82	this work
	VAL	$(2.56 \pm 0.10) \times 10^9$	2	4.52	this work
	CFA	$(3.37 \pm 0.22) \times 10^9$	2	3.43	this work
	ferulic acid	3.2×10^9	—	3.62	(Zhu et al., 2006)
	sinapic acid	3.2×10^9	—	3.62	(Zhu et al., 2006)
	syringic acid	$(1.7 \pm 0.1) \times 10^9$	3	6.81	(Tong et al., 2020)
$^{\bullet}OH$	VAA	$(9.8 \pm 1.5) \times 10^9$	2	1.29	(Tang et al., 2020)
	guaiacol	$(6.8 \pm 3.1) \times 10^9$	2	1.86	(Smith et al., 2015)
	syringol	$(1.7\pm 0.4) \times 10^{10}$	2	0.74	(Smith et al., 2015)
	syringaldehyde	3.70×10^{10}	2	0.34	(An et al., 2020)
	vanillyl alcohol	$(8.2 \pm 3.8) \times 10^9$	2	1.54	(Arciva et al., 2022)
	guaiacyl acetone	$(8.8 \pm 4.2) \times 10^9$	2	1.43	(Arciva et al., 2022)
	ferulic acid	$(13 \pm 6) \times 10^9$	2	0.97	(Arciva et al., 2022)
	syringic acid	$(9.4 \pm 4.4) \times 10^9$	2	1.34	(Arciva et al., 2022)
	syringyl acetone	$(14 \pm 7) \times 10^9$	2	0.90	(Arciva et al., 2022)
	5-methoxysalicylic acid	1.2×10^{10}	6-8	1.05	(O'neill and Steenken, 1977)
	3-methoxyphenol	2.2×10^{10}	6-7	0.57	(O'neill and Steenken, 1977)
	4-methoxyphenol	1.8×10^{10}	6-7	0.70	(O'neill and Steenken, 1977)
	3,5-dimethoxyphenol	1.5×10^{10}	6-7	0.84	(O'neill and Steenken, 1977)
	2,3-dimethoxyphenol	1.4×10^{10}	6-7	0.90	(O'neill and Steenken, 1977)
	creosol	$(1.7 \pm 0.4) \times 10^{10}$	5.6-6.0	0.74	(He et al., 2019)
	3-methoxycatechol	$(1.9 \pm 0.4) \times 10^{10}$	5.6-6.0	0.66	(He et al., 2019)
$^3C^*$	guaiacol	$(3.2 \pm 0.7) \times 10^9$	2	1.74	(Smith et al., 2015)
	syringol	$(6.7 \pm 1.5) \times 10^9$	2	0.83	(Smith et al., 2015)
	vanillyl alcohol	$(3.0 \pm 0.75) \times 10^9$	2	1.85	(Ma et al., 2021)
	guaiacyl acetone	$(3.3 \pm 0.83) \times 10^9$	2	1.68	(Ma et al., 2021)
	ferulic acid	$(3.4 \pm 0.85) \times 10^9$	2	1.63	(Ma et al., 2021)
	syringic acid	$(3.2 \pm 0.80) \times 10^9$	2	1.74	(Ma et al., 2021)
	syringyl acetone	$(4.5 \pm 1.1) \times 10^9$	2	1.23	(Ma et al., 2021)

742 [a] Atmospheric lifetime (τ) is calculated using average $SO_4^{\bullet-}$, $^{\bullet}OH$, and $^3C^*$

743 concentrations in atmospheric aqueous environment of 2.4×10^{-14} M (Herrmann et al.,

744 2010), 2.2×10^{-14} M (Herrmann et al., 2010), and 5.0×10^{-14} M (Kaur and Anastasio,

745 2018), respectively.

https://doi.org/10.5194/egusphere-2026-5353
Preprint. Discussion started: 29 September 2026

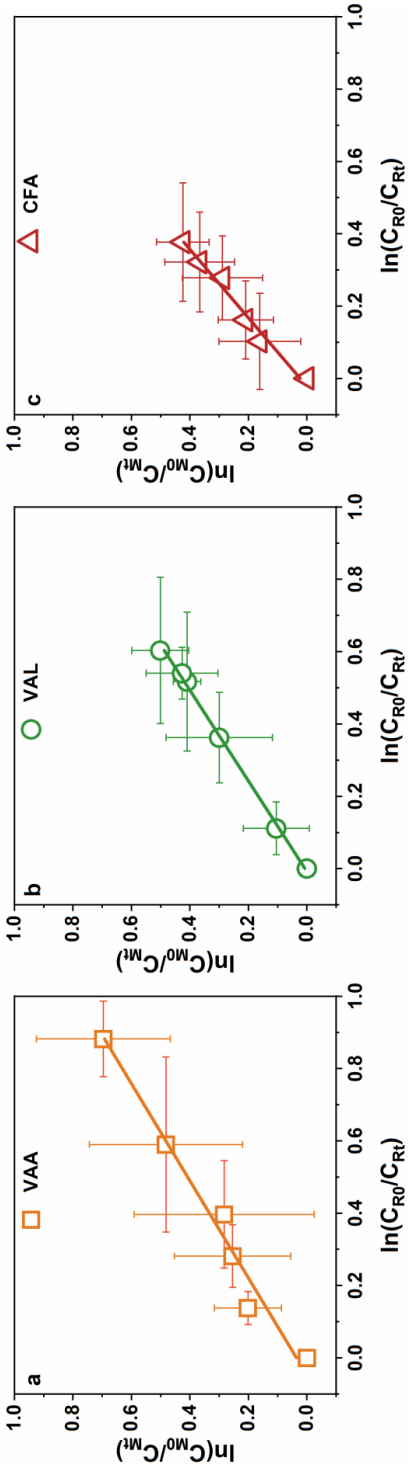

Figure 1. Plots of $\ln(C_{M0}/C_{Mt})$ versus $\ln(C_{R0}/C_{Rt})$ for aqueous-phase reactions of $SO_4^{\bullet-}$ with VAA (a), VAL (b), CFA (c), and reference compound (ferulic acid).

https://doi.org/10.5194/egusphere-2026-5353
Preprint. Discussion started: 29 September 2026

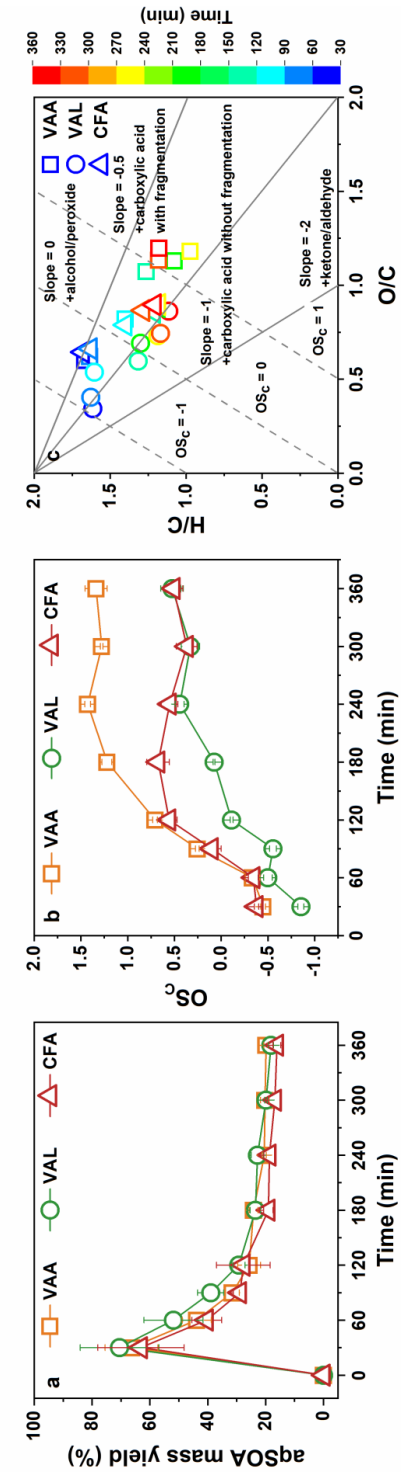

Figure 2. Time-series variations in aqSOA mass yields (a) and OS_C values (b) during aqueous-phase oxidation of VAA, VAL, and CFA by $SO_4^{\bullet-}$, and Van Krevelen diagram of the formed aqSOA (c).

https://doi.org/10.5194/egusphere-2026-5353
Preprint. Discussion started: 29 September 2026

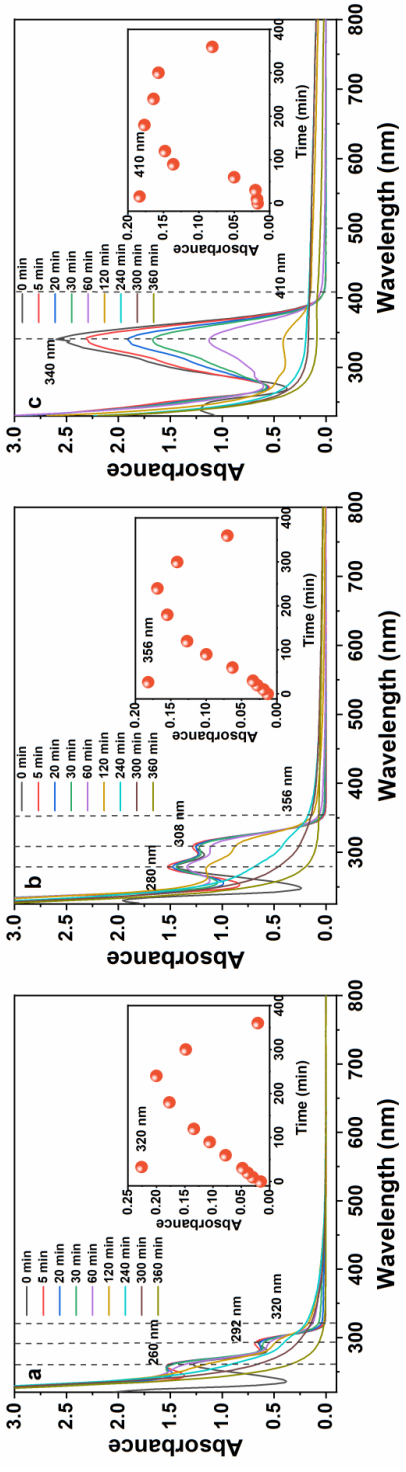

Figure 3. UV-vis absorption spectra of VAA (a), VAL (b), and CFA (c) in the aqueous-phase reactions with $SO_4^{\bullet-}$.

https://doi.org/10.5194/egusphere-2026-5353
Preprint. Discussion started: 29 September 2026

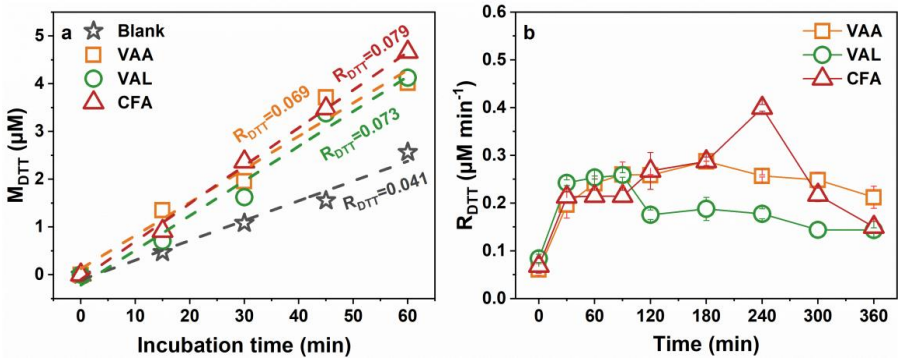

754

755 **Figure 4.** Correlation between DTT consumed mass (M_{DTT}) and incubation time (a),

756 and correlation between DTT consumption rate (R_{DTT}) and reaction time (b).